JOURNAL OF OPTOELECTRONICS AND ADVANCED MATERIALS Vol. 17, No. 9-10, September – October 2015, p. 1253 - 1257

Broadband second-harmonic generation in orientation-patterned GaAs

MING YIN*

School of Information Science and Technology, Chengdu University of Technology, Chengdu, 610059, China

The efficient broadband quasi-phase matching (QPM) second-harmonic generation (SHG) is investigated in orientation-patterned (OP) GaAs. Based on the theory of broadband QPM SHG, the group-velocity (GV) matching wavelength, corresponding QPM crystal grating period and SHG bandwidth are obtained at room temperature(25 °C). The influence of temperature on broadband QPM SHG are studied. The broadband QPM SHG behavior with the fundamental wave centered at 7, 9.24, 10 and 13 μm are discussed. For broadband QPM SHG, GV matching wavelength and corresponding QPM crystal grating period are 9.24 μm and 219.28 μm, SHG bandwidth are 744 nm for the crystal length is10 mm at room temperature. The SHG bandwidth decreases with deviation from central wavelength increasing, when the crystal length is10 mm, the SHG bandwidth are 31 and 60 nm with the fundamental wave centered at 7 and 13 μm at room temperature, respectively. The influence of temperature on GV matching wavelength and SHG bandwidth is little. The result can be used for broadband mid-infrared laser SHG with bandwidth several hundred or tens of nanometers.

(Received July 28, 2015; accepted September 9, 2015)

Keywords: Broadband; Quasi-phase matching; Second-harmonic generation; Orientation-patterned GaAs

1. Introduction

Due to a wide variety of applications like fiber communication, signal processing and spectroscopy, broadband QPM SHGs in periodically poled $LiNbO_3$(PPLN)[1-5], periodically poled $LiTaO_3$(PPLT)[6,7], periodically poled $KNbO_3$(PPKN)[8,9] and periodically poled $KTiOPO_4$(PPKTP)[10-12] have attracted much attention. However, the maximum transparent wavelengths of PPLN, PPLT, PPKN and PPKTP are less than 6 μm [6], some lasers' broadband SHG can't be realized with the fundamental wave centered above 6 μm in this crystals. GaAs crystal is widely used in optoelectronics.[13-15] The transparency of GaAs is from 0.9 to 17 μm [16]. Though GaAs is an isotropic material, OP GaAs has been fabricated with some method for QPM SHG[17-19]. The OP GaAs is reasonable crystal for broadband QPM SHG with the fundamental wave centered above 6 μm.

In this paper, we investigate the efficient broadband QPM SHG in OP GaAs. The theory of broadband QPM SHG is analyzed. The GV matching wavelength, corresponding QPM crystal grating period and SHG bandwidth are obtained at room temperature. The influence of temperature on broadband QPM SHG are studied. The broadband QPM SHG behavior with the fundamental wave centered at 7, 9.24, 10 and 13 μm are discussed to consider the wavelength range of broadband QPM SHG in OP GaAs. The result can be used for broadband mid-infrared laser SHG.

2. Theoretical analysis

For QPM SHG, the wave vector mismatch Δk can be expressed as[20]

$$\Delta k = k_s - 2k_f - \frac{2\pi}{\Lambda} \tag{1}$$

where k_s is the second-harmonic wave vector, k_f is the fundamental wave vector and Λ is the grating period of OP GaAs. To reach the efficient broadband QPM SHG , both QPM and GV matching must be satisfied, the wave vector mismatch need to fulfill conditions $\Delta k = 0$ and $\frac{d\Delta k}{d\lambda_f} = 0$.

When $\Delta k = 0$, Λ can be calculated as

$$\Lambda = \frac{\lambda_f}{2n_s - 2n_f} \tag{2}$$

where n_s is the refractive index of second-harmonic wave, n_f is the refractive index of fundamental wave and λ_f is the fundamental wavelength.

When Λ is determined by Equation (2), $\frac{d\Delta k}{d\lambda_f}$ can be calculated as

$$\frac{d\Delta k}{d\lambda_f} = \frac{4\pi(\frac{dn_s}{d\lambda_f} - \frac{dn_f}{d\lambda_f})\lambda_f - 4\pi(n_s - n_f)}{\lambda_f^{\,2}} \tag{3}$$

The refractive index of OP GaAs can be written as [16]

$$n(\lambda) = \sqrt{g_0 + \frac{g_1}{\lambda_1^{-2} - \lambda^{-2}} + \frac{g_2}{\lambda_2^{-2} - \lambda^{-2}} + \frac{g_3}{\lambda_3^{-2} - \lambda^{-2}}} \tag{4}$$

where $\lambda_1 = 0.4431307 + 0.000050564\Delta T$, $\lambda_2 = 0.8746453 + 0.0001913\Delta T - 4.882\times10^{-7}\Delta T^2$, $\lambda_3 = 36.9166 - 0.011622\Delta T$, $g_0 = 5.372514$, $g_1 = 27.83972$, $g_2 = 0.031764 + 4.350\times10^{-5}\Delta T + 4.664\times10^{-7}\Delta T^2$, $g_3 = 0.00143636$, ΔT is the deviation from the reference temperature 22 °C, the unit of λ is μm.

3. Results and discussion

For broadband QPM SHG, the grating period of OP GaAs and $\frac{d\Delta k}{d\lambda_f}$ are calculated at room temperature, as shown in Figure 1. The horizontal and vertical dash line represent $\frac{d\Delta k}{d\lambda_f}$=0 and corresponding λ_f. When $\frac{d\Delta k}{d\lambda_f}$=0, λ_f =9.24 µm and corresponding QPM grating period Λ =219.28 µm, QPM and GV matching are satisfied, the efficient broadband QPM SHG can be obtained with the fundamental wave centered at 9.24 µm and grating period Λ =219.28 µm at room temperature.

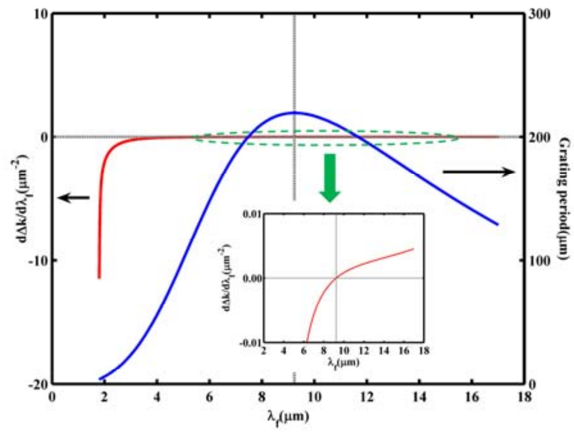

Fig. 1. The grating period and $\frac{d\Delta k}{d\lambda_f}$ as a function of the fundamental wavelength λ_f at room temperature

The refractive index depends on crystal temperature, so the GV matching λ_f is different at different temperature from equation(3). For QPM SHG, The GV matching λ_f and corresponding QPM grating period are calculated at different temperature, as shown in Figure 2. The GV matching λ_f increases less than 0.10 µm with temperature increasing from 22 to 95 °C. The influence of temperature on the GV matching λ_f is little.

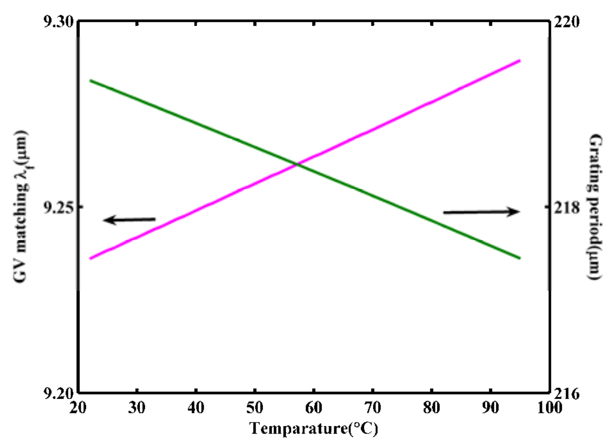

Fig. 2. The GV matching λ_f and corresponding QPM grating period as a function of temperature

The normalized SHG conversion efficiency η is proportional to $\mathrm{sinc}^2(\Delta kL/2)$, L is the crystal length. The SHG bandwidth is defined to be the λ_f variation at which η falls to half of its maximum value [21].

Fig. 3 shows the normalized SHG conversion efficiency η as a function of λ_f centered at 9.24 μm with corresponding QPM Λ =219.28 μm at room temperature. The SHG bandwidth are 744 nm, 525 nm, 429 nm and 372 nm for the crystal length L =10 mm, 20 mm, 30 mm, 40 mm, respectively. The SHG bandwidth decreases with the crystal length increasing. However, the conversion efficiency increases with the crystal length increasing. So the crystal length must be chosen according to practical needs.

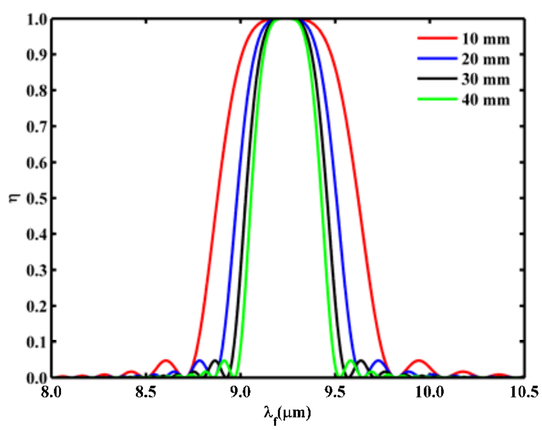

Fig. 3. The normalized SHG conversion efficiency η as a function of λ_f centered at 9.24 μm at room temperature

From Fig 2, the influence of temperature on the GV matching λ_f is little, the method of tuning GV matching λ_f by tuning temperature is of no use. However, from Fig. 1, $\frac{d\Delta k}{d\lambda_f}$ is near zero with the fundamental wave centered from 7 to 13 μm. Three fundamental wavelength ranges are considered to determine possible wavelength ranges of broadband QPM SHG without complete GV matching in OP GaAs.

Fig. 4 shows the normalized SHG conversion efficiency η as a function of λ_f centered at 10 μm with corresponding QPM Λ =216.78 μm at room temperature. The SHG bandwidth are 214 nm, 105 nm, 66 nm and 57 nm for the crystal length L =10 mm, 20 mm, 30 mm, 40 mm, respectively. The SHG bandwidth with the fundamental wave centered at 10 μm is less than one third of SHG bandwidth with the fundamental wave centered at GV matching wavelength 9.24 μm.

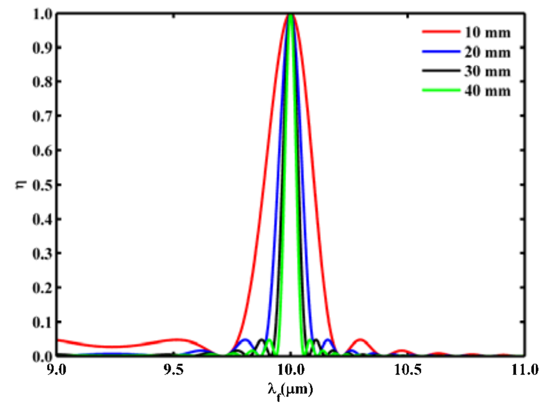

Fig. 4. The normalized SHG conversion efficiency η as a function of λ_f centered at 10 μm at room temperature

Fig. 5 shows the normalized SHG conversion efficiency η as a function of λ_f centered at 10 μm with corresponding QPM grating periods at different temperatures, the SHG bandwidth are nearly the same at 30, 40, 60 and 90 °C.

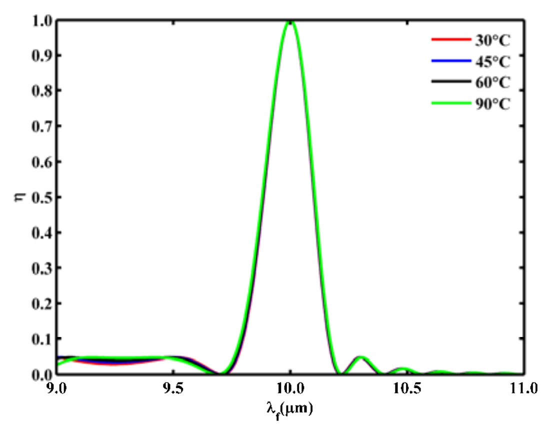

Fig. 5. The normalized SHG conversion efficiency η as a function of λ_f centered at 10 μm at different temperatures

Fig. 6 shows the normalized SHG conversion efficiency η as a function of λ_f centered at 13 μm with corresponding QPM grating period Λ =181.78 μm at room temperature . The SHG bandwidth are 60 nm, 40 nm, 20 nm and 20 nm for the crystal length L =10 mm, 20 mm, 30 mm, 40 mm, respectively. The SHG bandwidth falls to tens of nanometers.

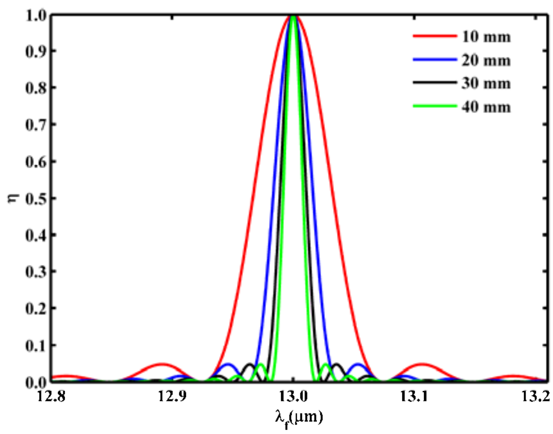

Fig. 6. The normalized SHG conversion efficiency η as a function of λ_f centered at 13 μm at room temperature

Fig. 7 shows the normalized SHG conversion efficiency η as a function of λ_f centered at 7 μm with corresponding QPM grating period Λ =186.71 μm at room temperature. The SHG bandwidth are 31 nm, 16 nm, 10 nm and 8 nm for the crystal length L =10 mm, 20 mm, 30 mm, 40 mm, respectively. The SHG bandwidth falls to tens of nanometers, even a few nanometers.

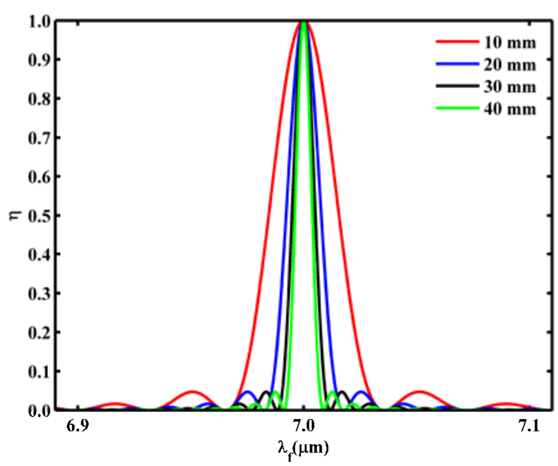

Fig. 7. The normalized SHG conversion efficiency η as a function of λ_f centered at 7 μm at room temperature

4. Conclusion

In conclusion, we have investigated broadband QPM SHG in OP GaAs with the fundamental wave centered from 7 to 13 μm. The GV matching wavelength and corresponding QPM grating period crystal grating period are obtained from 22 to 95 °C. The SHG bandwidth with the fundamental wave centered at 7, 9.24, 10 and 13 μm are discussed. For broadband QPM SHG, GV matching wavelength and corresponding QPM crystal grating period are 9.24 μm and 219.28 μm, SHG bandwidth are 744 nm for the crystal length is10 mm at room temperature. The influence of temperature on GV matching wavelength and SHG bandwidth is little. The SHG bandwidth decreases with the crystal length increasing. The SHG bandwidth decreases with deviation from central wavelength increasing, when the crystal length is10 mm, the SHG bandwidth are 31 and 60 nm with the fundamental wave centered at 7 and 13 μm, respectively. The result can be used for broadband mid-infrared laser SHG with bandwidth several hundred or tens of nanometers from 8 to 12 μm.

References

[1] N. E. Yu, J. H. Ro, M. Cha, S. Kurimura, T. Taira, Opt. Lett. **27**, 1046(2002)
[2] N. E. Yu, S. Kurimura, K. Kitamura, J. H. Ro, M. Cha, S. Ashihara, T. Shimura, K. Kuroda, T. Taira, Appl. Phys. Lett. **82**, 3388(2003)
[3] S. Ashihara, T. Shimura, K. Kuroda, J. Opt. Soc. Am. B **20**, 853(2003)
[4] J. Zhang, Y. Chen, F. Lu, W. Lu, W. Dang, X. Chen, Y. Xia, Appl. Optics **46**, 7791(2007)
[5] Z. Huang, C. Tu, S. Zhang, Y. Li, F. Lu, Y. Fan, E. Li, Opt. Lett. **35**, 877(2010)
[6] K. Lee, C. S. Yoon, F. Rotermund, Jpn. J. Appl. Phys. **44**, 1264(2005)
[7] S. Stivala, A. C. Busacca, A. Pasquazi, R. L. Oliveri, R. Morandotti, G. Assanto, Opt. Lett. **35**, 363(2010)
[8] N. E. Yu, S. Kurimura, K. Kitamura, O. Jeon, M. Cha, S. Ashihara, T. Ohta, T. Shimura, K. Kuroda, J. Hirohashi, Appl. Phys. Lett. **85**, 5839(2004)
[9] S. H. Bae, I. H. Beak, S. Y. Choi, W. B. Cho, F. Rotermund, C. S. Yonn, Opt. Commun. **283**, 1894(2010)
[10] F. Konig, F. N. C. Wong, Appl. Phys. Lett. **84**, 1644(2004)
[11] R. Wu, Y. Chen, J. Zhang, X. Chen, Y. Xia, Appl. Optics **44**, 5561(2005)
[12] F. Laurell, T. Calmano, S Muller, P. Zeil, C. Canalias, G. Huber, Opt. Express **20**, 22308(2012)
[13] F. Maskuriy, M. S. Alias, S. M. Mitani, A. A. Manaf, J. Optoelectron. Adv. Mater. **13**, 1213(2011)
[14] A. Rottler, M. Broll, N. Gerken, D. Heitmann, S. Mendach, Opt. Lett. **36**, 4797(2011)
[15] S. Buckley, M. Radulaski, J. L. Zhang, J. Petykiewicz, K. Biermann, J. Vuckovic, Opt. Lett. **39**, 5673(2014)

[16] T. Skauli, P. S. Kuo, K. L. Vodopyanov, T. J. Pinguet, O. Levi, L. A. Eyres, J. S. Harris, M. M. Fejer, B. Gerard, L. Becouarn, E. Lallier, J. Appl. Phys. **94**, 6447(2003)
[17] L. A. Eyres, P. J. Tourreau, T. J. Pinguet, C. B. Ebert, J. S. Harris, M. M. Fejer, L. Becouarn, B. Gerard, E. Lallier, Appl. Phys. Lett. **79**, 904(2001)
[18] C.Lynch, D. F. Bliss, T. Zens, A. Lin, J. S. Harris, P. S. Kuo, M. M. Fejer, J. Cryst. Growth **310**, 5241(2008)
[19] C.Lynch, D. F. Bliss, M. Snure, V. Tassev, G. Bryant, C. Yapp, D. B. Fenner, M. G. Allen, K. Termkoa, J. Li, S. Vangala, W. Goodhue, J. Cryst. Growth **353**, 152(2012)
[20] M. Yin, S. Zhou, G. Feng, Acta Phys. Sin. **61**, 234206(2012)
[21] Y. Chen, X. Chen, S. Xie, X. Zeng, Y. Xia, Y. Chen, J. Opt. A: Pure Appl. Opt. **4**, 324(2002)

*Corresponding author: yinmingcdut@163.com